





This file is an uncorrected accepted manuscript (i.e., postprint). Please be aware that this version will change during the production process. This postprint will be removed once the paper is officially published. All legal disclaimers that apply to the journal pertain.

Submitted: 30 April 2025 - Accepted: 24 September 2025 - Posted online: 3 October 2025

To link and cite this article:

doi: 10.5710/AMGH.24.09.2025.3642

PLEASE SCROLL DOWN FOR ARTICLE

- 1 AN ABELISAURID HUMERUS FROM THE BAJO DE LA CARPA
- 2 FORMATION (UPPER CRETACEOUS, SANTONIAN), NORTHERN
- 3 PATAGONIA, WITH COMMENTS ON MORPHOLOGICAL ASPECTS OF
- 4 THE HUMERUS IN ABELISAURIDAE

5

- 6 ARIEL H. MÉNDEZ¹, E. EMANUEL SECULI-PEREYRA¹, JAVIER GONZÁLEZ-
- 7 DIONIS¹, LUCÍA F. VETTORAZZI², ARIANA PAULINA-CARABAJAL^{3,4},
- 8 FEDERICO A. GIANECHINI², LEONARDO S. FILIPPI⁵, ALBERTO C. GARRIDO⁶,
- 9 MAGALÍ CÁRDENAS⁷, PENÉLOPE CRUZADO-CABALLERO^{8,9}, DO-KWON
- 10 KIM¹⁰, YUONG-NAM LEE¹¹

- ¹Instituto Patagónico de Geología y Paleontología (CCT CONICET-CENPAT), Bv.
- 13 Brown 2915, U9120ACD, Puerto Madryn, Chubut, Argentina.
- 14 arielhmendez@yahoo.com.ar
- ²Instituto Multidisciplinario de Investigaciones Biológicas de San Luis (CONICET-
- 16 UNSL), Ejército de Los Andes 950, D5700HHV, San Luis, San Luis, Argentina.
- ³Instituto de Investigaciones en Biodiversidad y Medioambiente (CONICET-
- 18 INIBIOMA-UNCo), Quintral 1250, R8400FRF, S. C. de Bariloche, Río Negro,
- 19 Argentina.
- ⁴Museo Paleontológico Bariloche. 12 de Octubre y Sarmiento, 8400, San Carlos de
- 21 Bariloche, Río Negro, Argentina.
- ⁵Museo Municipal "Argentino Urquiza", Chos Malal 1277, Q8319AVY, Rincón de los
- 23 Sauces, Neuquén, Argentina.

- ⁶Museo Provincial de Ciencias Naturales "Prof. Dr. Juan Olsacher", Dirección
- 25 Provincial de Minería, Etcheluz y Ejército Argentino, Q8340AUB, Zapala, Neuquén,
- 26 Argentina.
- ⁷Museo Argentino de Ciencias Naturales "Bernardino Rivadavia", Av. Ángel Gallardo
- 28 470, C1405DJR, Ciudad de Buenos Aires, Argentina
- 29 ⁸Área de Paleontología, Universidad de La Laguna, Av. Astrofísico Francisco Sánchez,
- 30 s/n, La Laguna, Tenerife, España.
- 31 ⁹ Grupo Aragosaurus-IUCA, Facultad de Ciencias, Universidad de Zaragoza, C/ Pedro
- 32 Cerbuna, 12, 50009 Zaragoza, Spain.
- 33 ¹⁰Sicheong-ro, Namyang-eup, Hwaseong-si, Gyeonggi-do 18274, Republic of Korea.
- 34 ¹¹School of Earth and Environmental Sciences, Seoul National University, Seoul 08826,
- 35 Republic of Korea.

36

38

43

45

46

47

- 37 28 pag. (text + references); 6 figs.; 1 table
- 39 Running Header: MÉNDEZ ET AL.: ABELISAURID HUMERUS FROM
- 40 PATAGONIA
- 41 Short Description: A new humerus of Abelisauridae is described. It displays
- 42 morphological characteristics intermediate between noasaurids and derived abelisaurids.
- 44 Corresponding author: Ariel Hernán Méndez <u>arielhmendez@yahoo.com.ar</u>

49 **Abstract.** The Cerro Overo-La Invernada área (Bajo de la Carpa Formation, Upper 50 Cretaceous, Santonian) in northern Patagonia has yielded abundant fossils of abelisaurid 51 theropods, including cranial, vertebral, pectoral and pelvic remains. However, forelimb 52 bones were unknown. Here, we describe a humerus that exhibits distinctive features that 53 allow its assignment to Abeliauridae, for example, flattened distal condyles, greater 54 tubercle distally located, and humeral head subspherical in proximal view. It also 55 exhibits a noticeable torsion of the distal end. Morphofunctional analysis indicates a 56 substantial capacity for protraction along with a limited capacity for lateromedial 57 movement. In a general aspect, MAU-PV-LI-737 is morphologically intermediate 58 between the more gracile humerus of noasaurids and the robust shape observed in 59 Campanian-Maastrichtian abelisaurid forms. 60 **Keywords.** Humerus. Abelisauridae. Bajo de la Carpa Formation. Upper Cretaceous. 61 Geometric morphometric. Resumen. UN HÚMERO DE ABELISÁURIDO DE LA FORMACIÓN BAJO DE LA 62 63 CARPA (CRETÁCICO SUPERIOR, SANTONIANO), PATAGONIA NORTE, CON COMENTARIOS SOBRE ASPECTOS MORFOLÓGICOS DEL HÚMERO EN 64 65 ABELISAURIDAE. El área Cerro Overo-La Invernada (Formación Bajo de la Carpa, 66 Cretácico Superior, Santoniano) en el norte de la Patagonia ha producido abundantes 67 fósiles de terópodos abelisáuridos, incluyendo restos craneales, vertebrales, pectorales y pélvicos. Sin embargo, se desconocían huesos de las extremidades anteriores. Aquí 68 describimos un húmero que exhibe características distintivas que permiten su 69 70 asignación a Abelisauridae, por ejemplo, cóndilos distales aplanados, tubérculo mayor 71 distalmente ubicado, cabeza humeral subesférica en vista proximal. También exhibe una 72 notable torsión del extremo distal. El análisis morfofuncional indica una considerable 73 capacidad de protracción junto con una limitada capacidad de movimiento lateromedial.

74	En aspecto general, MAU-PV-LI-737 es morfológicamente intermedio entre el húmero
75	más grácil de los noasáuridos y la forma robusta observada en los abelisáuridos del
76	Campaniano-Maastrichtiano.
77	Palabras clave. Húmero. Abelisauridae. Formación Bajo de la Carpa. Cretácico
78	Superior. Morfometría geométrica.
79	
80	
81	
82	
83	
84	
85	
86	
87	
88	
89	
90	
91	
92	
93	
94	
95	
96	
97	

CERRO OVERO – LA INVERNADA IS A PROLIFIC FOSSILIFEROUS AREA where Cretaceous sediments from the Bajo de la Carpa, Anacleto, and Allen formations emerge. Among these, the Bajo de la Carpa Formation stands out for the abundance and diversity of vertebrate fossils discovered, which include sauropod, theropod, and ornithopod dinosaurs, crocodiles, turtles, fish, as well as dinosaur footprints and eggs (Cruzado-Caballero et al., 2018, 2019; Filippi et al., 2016, 2018, 2024; Gianechini et al., 2021, 2022; Jiménez-Gomis et al., 2018; Méndez et al., 2018, 2022, 2024; Panzeri et al., 2022; Paulina-Carabajal et al., 2024). The remains of abelisauroid theropods, along with titanosaurid sauropods and chelid turtles, represent the largest number of specimens. To date, nine specimens belonging to the family Abelisauridae have been recovered, including two named taxa (Viavenator and Llukalkan, Filippi et al., 2016; Gianechini et al., 2021), four undetermined ones, and three others under study. All these forms can be nested within the clade Brachyrostra, except one (Gianechini et al., 2022) within Furileusauria. Among abelisaurid theropods from the Bajo de la Carpa Formation, forelimb elements are scarce, represented solely by the scapulocoracoid of *Viavenator*. The humerus in Abelisauroidea is characterized by an anteroposterior expansion of the humeral head, a reduced development of the deltopectoral crest, the presence of a posterior or lateroposterior tuberosity, and a distal end with flattened radial and ulnar condyles. Noasaurids have a more slender humerus within this clade whereas abelisaurids tend to have a more robust and shorter humerus relative to body size (Novas et al., 2006; Méndez et al., 2010; Burch & Carrano, 2012). Classical morphological studies are currently complemented by analysis using Geometric Morphometrics (GM), a tool that allows for evaluating shape changes (Zelditch et al., 2004; Benítez & Püschel, 2014). Combined with statistical analyses and descriptive graphics, GM enables effective quantification and a more appropriate

98

99

100

101

102

103

104

105

106

107

108

109

110

111

112

113

114

115

116

117

118

119

120

121

123	interpretation of morphological variation (Adams et al., 2013). In this work, we
124	describe the tenth abelisaurid specimen for the Cerro Overo-La Invernada area (Figure
125	1), corresponding to a left humerus (Figure 2) exhibiting morphological features linked
126	to the Abelisauridae family. We combined geometric morphometric techniques and
127	statistical analyses to describe the shape variation and morphological affinities of this
128	material. Additionally, we tested whether the differences in the humerus shape could be
129	explained by taxonomical group and allometry.
130	Institutional abbreviations. FMNH, Field Museum of Natural History, Chicago, USA;
131	ISI, Indian Statistical Institute, Kolkata, India; MACN, Museo Argentino de Ciencias
132	Naturales "Bernardino Rivadavia", Buenos Aires, Argentina; MAU, Museo Municipal
133	"Argentino Urquiza", Rincón de los Sauces, Argentina; MB, Museum fur Naturkunde
134	Berlin, Germany; MCF, Museo "Carmen Funes", Plaza Huincul, Argentina. MPCN,
135	Museo Patagónico de Ciencias Naturales, General Roca, Argentina; MPCO, Museu de
136	Paleontologia de Cruzeiro do Oeste, Cruzeiro do Oeste, Brazil
137	Anatomical abbreviations. dc, deltopectoral crest; gt, greater tubercle; hh, humeral
138	head; it, internal tuberosity; n, notch; pt, posterior tuberosity; rc, radial condyle; uc,
139	ulnar condyle
140	MATERIALS AND METHODS
141	Material
142	MAU-Pv-LI-737: complete left humerus.
143	Methods
144	Sample data and geometric morphometrics. Jointly with the humerus MAU-PV-LI-
145	737, two-dimensional (2D) published left humeri images and photographs in anterior
146	view were used. A total of four abelisaurids (Carnotaurus (personal image),
147	Eoabelisaurus (personal image), Majungasaurus (Carrano, 2007; Burch & Carrano,

148 2012) and Aucasaurus (Coria et al., 2002), three noasaurids (Elaphrosaurus, Rauhut & 149 Carrano, 2016; Masiakasaurus, Carrano et al., 2011; and Vespersaurus, Langer et al., 150 2019), one early diverging ceratosaurid (*Ceratosaurus*, Madsen & Welles, 2000) and 151 one early diverging tetanuran (Allosaurus, Madsen, 1976) were used. When only the 152 right element was available, we mirrored the image to allow landmarking. We designed 153 a 2D configuration for the anterior view with five landmarks and 27 semilandmarks, 154 digitized in tpsDig (2.6.4; Rohlf, 2004) (Figure 3-2 and Supplementary Online 155 Information; Table 1). Likewise, we designed a 2D configuration to proximal view with 156 two landmarks and 14 semilandmarks (Figure 4-2 and Supplementary Online 157 Information, Table 2). Finally, a Generalized Procrustes Analysis was performed to 158 eliminate the effects of rotation, translocation, and scale, obtaining the shape and size 159 variables that were used for downstream analyses (gpagen, geomorph package; Adams 160 & Otárola-Castillo, 2013) in both humeri views. 161 Ordination methods (Principal Component Analysis) and hypothesis testing. 162 Ordination methods reduce the number of shape variables into a few principal 163 components, which describe the significant shape changes across the morpho-space. We 164 performed a Principal Component Analysis (PCA) (gm.prcomp function, geomorph 165 package) to describe the significant shape changes across our humeri sample, 166 emphasizing the shape changes of MAU-PV-LI-737. 167 We tested whether the differences in humeri shape could be explained by 168

We tested whether the differences in humeri shape could be explained by taxonomical group (Abelisauridae, Noasauridae, and early diverging taxa or outgroups), allometry (Centroid Size based), and the cross-factor (the interaction between these variables) using a Procustes ANOVA (procD.lm function, geomorph and RRPP package; Collyer & Adams, 2018) in the Procustes Coordinates (PC). Additionally, since Procustes Coordinates represents all the variation in humeri shape data, we also

169

170

171

173	used 90% of PC components in order to avoid more variables (numbers of landmarks)
174	than species in the analysis.
175	Finally, since statistics based on the overconfidence in P-values has mainly been
176	criticized (Benjamin et al., 2018; Amrhein et al., 2019; Yang et al., 2023), we used the
177	variance explained (R-squared) and effect size (standardized differences (Z)) estimated
178	in the Procustes ANOVA to discuss our results more compressively.
179	Osteological correlates and musculature. The osteological correlates and muscle
180	nomenclature used in this study follow the work of Burch (2017), who performed a
181	detailed myological reconstruction of the forelimb of the abelisaurid Majungasaurus
182	crenatissimus. The abbreviations used for muscles (e.g., M. subscapularis (SBS), M.
183	latissimus dorsi (LD), M. coracobrachialis (CB)) are consistent with the standardized
184	format proposed in that work, which integrates the extant phylogenetic bracket (EPB;
185	Witmer, 1995) with osteological correlates to infer soft tissue anatomy in non-avian
186	theropods.
187	
188	SYSTEMATIC PALEONTOLOGY
189	THEROPODA Marsh, 1881
190	CERATOSAURIA Marsh, 1884
191	ABELISAUROIDEA Bonaparte, 1991
192	ABELISAURIDAE Bonaparte & Novas, 1985
193	Abelisauridae indet.
194	
195	Type material. MAU-Pv-LI-737 Left humerus
196	Geographic occurrence. La Invernada fossil site, 50 km south of Rincón de los Sauces
197	city, Neuquén province, Argentina

198 **Stratigraphic occurrence.** Bajo de la Carpa Formation (Santonian, Upper Cretaceous) 199 **Description.** The humerus (MAU-Pv-LI-737) is complete and measures 18.5 cm. The 200 humeral head is oval in proximal view, with the main axis in lateromedial direction, 201 similar to Eoabelisaurus (Pol & Rauhut, 2012), Elaphrosaurus (Janensch, 1920), 202 Vespersaurus (Langer et al., 2019) and the abelisauroid MCF-PVPH 53 (Novas et al., 203 2006), and unlike the rounded and globose shape observed in *Carnotaurus* (Bonaparte, 204 1985), Majungasaurus (Lavocat, 1955), Aucasaurus (Coria et al., 2002), Rahiolisaurus 205 (Novas et al., 2010), and MPCN-PV 69 (Gianechini et al., 2015). In posterior view, the 206 distal margin of the humeral head is located above the level of the internal tuberosity, as 207 seen in Eoabelisaurus, Elaphrosaurus, Masiakasaurus (Sampson et al., 2001), 208 Vespersaurus, Majungasaurus, Aucasaurus and MCF-PVPH 53, but unlike 209 Carnotaurus and MPCN-PV 69, in which the distal margin is at the same level as the 210 internal tuberosity. The deltopectoral crest and greater tubercle are less developed than 211 in other abelisaurids and noasaurids. The internal tuberosity is separated from the 212 humeral head by a poorly marked notch, similar to that observed in Majungasaurus, 213 Rahiolisaurus, Elaphrosaurus, and MCF-PVPH-53. In contrast, Aucasaurus, 214 Carnotaurus, and MPCN-PV 69 exhibit a more conspicuous notch. In MAU-Pv-LI-737, 215 as in Aucasaurus, Carnotaurus, Majungasaurus, Rahiolisaurus, and MPCN-PV-69, the 216 internal tuberosity is located above the level of the greater tubercle, whereas in the basal 217 abelisauroid MCF-PVPH-53 is located at the same level. On the other hand, in 218 Elaphrosaurus and Vespersaurus, the internal tuberosity is located below the level of 219 the greater tubercle. The diaphysis is wide and arched, in anterior and posterior views, 220 as in several abelisaurids such as Carnotaurus, Aucasaurus, and Majungasaurus, 221 whereas in noasaurids such as *Elaphrosaurus*, *Vespersaurus*, and *Masiakasaurus*, the 222 diaphysis is less arched and narrower. However, MAU-Pv-LI-737 differs because the

223 diaphysis in its distal third shows a rotation that makes the ulnar condyle remain in an 224 anteromedial position instead of medial. Furthermore, a slight notch can be seen 225 between the radial and ulnar condyles in the distal view, similar to that seen in 226 Majungasaurus, Vespersaurus, and Elaphrosaurus. On the other hand, in Aucasaurus, 227 this notch is much more noticeable whereas it is not observed in Carnotaurus and 228 Masiakasaurus. In the anterior view, just below the edge of the humeral head, a slight 229 depression is observed, possibly representing the insertion area for the M. 230 coracobrachialis (Jasinoski et al., 2006; Carrano, 2007; Burch, 2017). This shallow 231 condition is present in the abelisauroid MCF-PVPH 53 and Vespersaurus, which 232 contrasts with the marked groove present in Carnotaurus, Aucasaurus, Majungasaurus, 233 Rahiolisaurus and MPCN-PV 69, which is a product of the expansion of the humeral 234 head in an anteroposterior direction. In the posterior view, a poorly developed posterior 235 tuberosity is present at the level of the first proximal third. This bump is also present in 236 Aucasaurus, Carnotaurus, Majungasaurus, Rahiolisaurus, MPCN-PV 69, MCF-PVPH 237 53, and probably in *Ceratosaurus* (Burch, 2017). The presence of this structure, 238 possibly for the insertion of the M. latissimus dorsi and part of the M. deltoideus 239 (Jasinoski et al., 2006; Carrano, 2007), is not documented in Masiakasaurus, 240 Vespersaurus, and non-abelisauroid theropods (e.g., the coelophysoids Syntarsus and 241 *Liliensternus*, basal tetanurans as *Baryonyx*, *Allosaurus*, and in *Deinonychus*). 242 **RESULTS** 243 Ordination methods (Principal Component Analysis) and hypothesis testing 244 **PCA** in anterior view. The first two components of the PCA explained 64,69% of the 245 total variance of the data (Figure 3-1). The PC1 was related to the humeral head and the 246 internal tuberosity. This component distinguished Abelisauridae and early diverging 247 taxa from Noasauridae in a pronounced well-developed internal tuberosity and rounded

humeral head (Figure 3-1). The PC2 was related to the width and length of the humerus (Figure 3-1). This component distinguished abelisaurids from early diverging taxa and noasaurids in a short and wide humeral shape for abelisaurids. MAU-PV-LI-737 was found close to Late Cretaceous abelisaurid forms, being more similar to *Majungasaurus* in shape (Figure 3-1).

We found that the humeral size (centroid size) had little effect on the shape of the humerus in both data sets (Table 1). Moreover, the interaction between factors (Taxonomy*Size) in all datasets explained around 15% of the total variation. However, the taxonomy variable explained more than 30% of the total variation of the humeral shape in both data sets (Table 1).

PCA in proximal view. The first two components of the PCA explained 65,76% of the total variance of the data in the proximal view (Figure 4-1). The PC1 component was related to the shape of the humeral head. This component distinguishes Late Cretaceous abelisaurids from Noasauridae, *Eoabelisaurus*, and MAU-PV-LI-737 in a circular-shaped humeral head. The PC 2 was related to the lower edge between the internal tuberosity and the deltopectoral crest. This component distinguished Noasauridae from *Eoabelisaurus* and upper Cretaceous abelisaurids, in a concave-shaped edge. MAU-PV-LI-737 was found more closely to MPCN-PV-69 and MCF-PVPH-53.

Hypothesis testing. The presence of allometry in humeral shape and its correlation with taxonomic groups were evaluated within a quantitative framework using Procrustes ANOVA on Procrustes coordinates and in the 90% shape variation in the principal component analysis for both humerus views. Our results indicate that humerus size (centroid size) had only a minor effect on shape variation in both datasets and views (Table 1). Additionally, in both views, the interaction between taxonomy and size accounted for approximately 15% of the total shape variation across datasets. In

contrast, taxonomy alone explained over 30% of the total variation in humeral shape in both datasets and humerus views (Table 1).

Osteological correlates and functional morphology

273

274

275

276

277

278

279

280

281

282

283

284

285

286

287

288

289

290

291

292

293

294

295

296

297

The degree of preservation of this material allows inferences to be drawn about the development of the musculature in the humerus thanks to the bone correlates found in MAU-Pv-LI-737 (Fig. 5). The bone correlates described by Burch (2017) have been taken as a reference. The internal tuberosity (IT), medially directed and moderately developed, would be unequivocally the insertion zone of the M. subcoracoideus (SBC) in the anteromedial surface and of the M. subscapularis (SBS) in the posteromedial surface of the IT. However, the division where these two muscles would be attached, which is defined in other abelisaurids by an intermediate ridge (Burch, 2017), is not observed in MAU-Pv-LI-737, so its arrangement could not be precisely defined. The rugosity that indicate the attachment area of the M. scapulohumeralis posterior (SHP) is not present, although in this area is observed a slight depression. This area is unequivocally located posteriorly under the insertion zone of M. subscapularis in the internal tuberosity. In anteromedial view, there is a slight depression which would be the origin of the M. biceps brachii (BB). The slight depression under the humeral head in the anterior view would be the insertion zone of the M. coracobrachialis (CB). Similarly, we can observe the slight development of the insertion zone of the supracoracoideus complex, which is formed by two muscles, the M. supracoracoideus accessorius (SCA), which inserts in the anterior zone of the greater tubercle, where a slight roughness is observed, and the M. supracoracoideus (SC) which attaches in the distal zone of the deltopectoral crest. In the posterior view, there is a roughness in the greater tubercle where the M. deltoideus scapularis (DS) would insert. Towards the medial area, there is an anterolateral thickening of the deltopectoral crest, where the M.

pectoralis (P) would attach. The M. deltoideus clavicularis (DC) would attach on the lateral surface of the deltopectoral crest, where a wide striated area extending dorsoventrally over a concave surface is observed. The arrangement of the M. latissimus dorsi (LD) would be more displaced towards the more posteromedial area, taking the more medial location of the posterior tuberosity as a reference, although it is impossible to identify any depression to confirm this. This position makes the area of origin of the M. triceps brachii medialis (TBM) smaller, which could affect the extension of the forearm. In the posterolateral view, a groove can be seen corresponding to the tentative area of origin of the lateral M. triceps brachii lateralis muscle. The M. brachialis (BR) does not have any defined scars, making it difficult to establish its area of origin with certainty. However, it should have been attached to the anterior surface next to the distal area of the deltopectoral crest. This suggests that it would have a more medial location, since the distal area of the deltopectoral crest is not very developed. Distal musculature related to antebrachium articulation is inferred to originate in association with the entepicondyle and ectepicondyle, but these structures are difficult to differentiate. It should be noted that due to the torsion of the shaft, a large groove is observed in the posterodistal area where the insertion zone of the M. supinator (SU) would be located. Furthermore, in the anterior view near the ulnar condyle, small depressions are observed, one towards the more medial side and the other more distal, which could be indicative of the origin of the M. pronator teres (PT) and M. epitrocheloanconeus (EA), M. flexor carpi ulnaris (FCU) and M. flexor digitorum longus superficialis (FDLS), respectively.

DISCUSSION

298

299

300

301

302

303

304

305

306

307

308

309

310

311

312

313

314

315

316

317

318

319

320

321

322

Humeral features. Although MAU-Pv-LI-737 consists solely of a humerus, the general morphology of this bone demonstrates similarities with theropods belonging to the

324 recent phylogenetic analyses are discussed below. 325 Shape of the humeral head in proximal view (Rauhut, 2003). Rauhut (2003) identified 326 two states for this character: those that were markedly oval (more than twice as wide as 327 they were long anteroposteriorly) as in most theropods, and those that were more 328 rounded or not so oval, a shape present in *Elaphrosaurus* and abelisaurids. In 2016, 329 Rauhut and Carrano divided the latter state of the character into slightly oval (less than 330 twice as wide as long) and globose. This differentiation groups MAU-Pv-LI-737 with 331 the elaphrosaurins Masiakasaurus and Elaphrosaurus, as well as the basal abelisauroid 332 MCF-PVPH-53 (and probably also *Eoabelisaurus*). On the other hand, the globose 333 character is restricted to the majungasaurines Majungasaurus and Rahiolisaurus and the 334 brachyrostrans Carnotaurus, Aucasaurus, and MPCN-PV-69. The globose morphology 335 seems to be restricted to the abelisaurid taxa of the end of the Late Cretaceous 336 (Campanian-Maastrichtian). 337 Shape of distal humeral condyles (Carrano et al., 2002). Carrano and colleagues (2002) 338 identified the distal shape of the humerus with two well-defined states, rounded or 339 flattened condyles. The condyles, articulating with the radius and ulna, are rounded in 340 most theropods. However, they become more flattened in Ceratosauria (including 341 MAU-PV-LI-737), except in *Eoabelisaurus* and *Vespersaurus* (being less pronounced 342 in the latter), which appear to retain the plesiomorphic condition. 343 Placement of humeral greater tubercle (Sereno et al., 2004). The greater tubercle is 344 located approximately at the level of the humeral head in most theropods. In basal 345 abelisauroids and noasaurids (e.g., Vespersaurus, Elaphrosaurus, Masiakasaurus, 346 MCF-PVPH-53), it is located just below the level of the distal margin of the humeral

Abelisauridae clade (Figure 6). Characters associated with the humerus in the most

347	head. The greater tubercle is located more distally in MAU-PV-LI-737 and the rest of
348	the Abelisauridae.
349	Posterolateral tubercle on the proximal part of the humerus (Novas et al., 2006). Novas
350	and colleagues (2006) identified a bulge in the posterior sector of the humerus MCF-
351	PVPH-53. This feature is also present in MAU-PV-LI-737, the remaining abelisaurids,
352	and Elaphrosaurus, being absent in coelophysoids and basal tetanurans (Novas et al.,
353	2006).
354	Humerus in the anterior view (Rauhut & Carrano, 2016). Rauhut and Carrano (2016)
355	describe a new character in which the medial and lateral margins of humeri of non-
356	abelisauroid theropods would be concave or concave-straight, while in MAU-PV-LI-
357	737 and Abelisauroidea, the lateral margin is moderately convex and the medial one
358	markedly concave. This state of the character is not present in the noasaurin
359	Vespersaurus, which presents a more plesiomorphic condition.
360	Longitudinal torsion of humeral shaft (Holtz, 2000). In basal theropods, the proximal
361	and distal humeral articular surfaces are virtually in the same plane. A rotational axis
362	shift is observed in more derived forms (e.g., tetanurans, ceratosaurs; Carrano &
363	Sampson, 2008), resulting in a longitudinal torsion. It is slightly noticeable in
364	abelisaurids, while in MAU-PV-LI-737 and Elaphrosaurus, this rotation is more
365	pronounced.
366	Size of deltopectoral crest (Paul, 1984). Most theropods (and dinosaurs generally,
367	Benton, 1990; Sereno, 1999) have a well-developed deltopectoral crest. The
368	development of this structure is markedly diminished in MAU-PV-LI-737 and all
369	members of the Abelisauroidea.
370	Connection between the humeral head and the internal tuberosity, anterior view
371	(Gianechini et al., 2015). In 2015, Gianechini and colleagues identified a new character

372 related to the connection between the humeral head and the internal tuberosity. 373 Regardless of the morphology of the internal tuberosity (triangular or rectangular, 374 Rauhut, 2003), in Theropoda, it is continuous with the humeral head. In *Ceratosaurus*, 375 noasaurids, and majungasaurins (it also appears to be present in spinosaurids, Charig & 376 Milner, 1997), this transition is observed as a slight concavity, while in late diverging 377 furileusaurs such as Carnotaurus and Aucasaurus, a more pronounced step is seen. 378 Herrerasaurus presents an autapomorphic condition with a deep groove separating the 379 humeral head from an internal tuberosity. 380 **Morphofunctional inferences.** Based on the morphology of the osteological correlates 381 observed, it is possible to suggest that MAU-Pv-LI-737 should not have a great capacity 382 for protraction (muscles CB, DS, P, DC), being more similar to *Elaphrosaurus*. 383 Similarly, the moderate development, as seen in *Aucasaurus*, and the lack of 384 delimitation of the insertion area of SBS and SBC could indicate a low capacity for 385 adduction and medial rotation in humeral retraction, compared to other abelisaurids 386 such as Majungasaurus or Carnotaurus. The origin area of BR is similar to early 387 diverging theropods, where its tentative location would be more medial than in other 388 abelisaurids such as Majungasaurus or Carnotaurus, where it would be located slightly 389 more distally (Burch, 2014, 2017). Similarly, the distal musculature correlates are 390 poorly developed, which, combined with the flat morphology of the condyles, would 391 suggest poor pronation and supination capacity. Finally, comparative evidence in other 392 abelisaurids and theropods shows that humeral head morphology constrains shoulder 393 range of motion. In abelisaurids with bulbous and hemispherical head (e.g., 394 Carnotaurus, Majungasaurus), greater mobility is inferred, notably wide humeral 395 elevation in the transverse plane. In *Majungasaurus* this condition is explicitly 396 associated with broad shoulder ranges of motion, and in Carnotaurus it has been linked

to expanded elevation relative to theropods lacking a hemispherical head (Senter & Parrish, 2006; Burch, 2017). By contrast, in theropods with non-hemispherical heads the range of motion can be more restricted or asymmetric. For example, in *Acrocanthosaurus* the head is more posteriorly extensive (non-hemispherical), which favours greater retraction than protaction (Senter & Robins, 2005). Alternatively, some clades achieve high elevation whit a head offset toward the deltopectoral crest (non-hemispherical), as in *Mononykus*, maintaining glenoid contact over a wider arc (Senter, 2023). In this way, the oval morphology of the humeral head of MAU-Pv-LI-737 suggests a limitation in lateromedial movements compared to other abelisaurids with a bulbous and hemispherical humeral head.

CONCLUSIONS

The humerus of abelisauroid theropods is well represented by the abelisaurids

Carnotaurus, Majungasaurus, Aucasaurus, and the noasaurids Masiakasaurus,

Elaphrosaurus and Vespersaurus. However, this bone is not entirely known for more basal abelisaurid forms. The humerus described here adds new data on the forelimb morphology of this group of ceratosaurian theropods.

This material is interpreted as belonging to an indeterminated abelisaurid theropod, an assignment supported by a moderately inflated humeral head, a reduced deltopectoral crest, and posterior tuberosity on the humeral shaft. The condition of the humeral head in MAU-PV-LI-737 seems to be more primitive than the globose shape of *Majungasaurus, Rahiolisaurus, Aucasaurus*, and *Carnotaurus*, but more derived than in non-abelisauroid theropods. The slightly concave transition between the humeral head and the internal tuberosity is shared with other non-furileusaurian abelisauroids. MAU-PV-LI-737 shares with other abelisaurids the general curvature of the shaft in the anterior or posterior view. The location of the greater tubercle to the humeral head is

another characteristic that groups it with the Abelisauridae. However, MAU-PV-LI-737 does not share a marked torsion of the distal part of the shaft with other abelisauroids.

422

423

424

425

426

427

428

429

430

431

432

433

434

435

436

437

438

439

440

441

442

443

444

445

446

The osteological correlates and associated musculature observed in MAU-Pv-LI-737 suggest a limited functionality of the humerus, primarily restricted in protraction, adduction, and medial rotation, being morphologically located between noasaurids and derived abelisaurids. In addition, the oval shape of the humeral head implies restrictions in lateromedial movements. Future studies, will allow a more precise exploration of the muscular arrangement and functional capabilities of this abelisauroid forelimb.

Regarding GM and statistical analysis, the shape, in the anterior view, of MAU-PV-LI-737 is more similar to Campanian-Maastrichtian abelisaurids, with a robust humeral shape. However, the shape in proximal view was morphologically more similar to the Jurassic abelisaurid *Eoabelisaurus* and noasaurids. Therefore, in general aspect, MAU-PV-LI-737 seems to be morphologically intermediate between the more gracile humerus of noasaurids (e.g., Vespersaurus, Elaphrosaurus, Masiakasaurus) and the robust shape of derived abelisaurid forms (e.g., Majungasaurus, Carnotaurus, Aucasaurus). On the other hand, the taxonomical classification of taxa explained better the shape of the humerus than size and the interaction between these factors (Taxonomy and Size). It means that abelisaurids, especially late diverging abelisaurids, exhibit a characteristic and conservative morphology, within the members of the family. It is interesting to note that the most robust form is present in those taxa or specimens originating from Campanian-Maastrichtian strata, regardless of the group to which they belong within Abelisauridae (Brachyrostra + Majungasaurinae). Whereas less robust forms are found among pre-Campanian abelisaurids, the most gracile ones appear within noasaurids.

447 However, the present analysis lacks a phylogenetic comparative approach to 448 determine macroevolutionary patterns and trends in Abelisauridae humeral evolution. 449 Future research must consider a phylogenetic approach to determine what patterns of 450 evolution rates, selection strength, and constraint explain the conservative morphology 451 of the abelisaurid humerus. 452 **ACKNOWLEDGMENTS** 453 Paleontological fieldwork in La Invernada was carried out with financial support of 454 CONICET PIP 2021-2023 11220200101108CO (AHM); AGENCIA I+D+i PICT 2021-455 00024 (AHM), PICT-2021-00513 (LSF), PICT-2021-1053 (APC); Sepkoski Grant 2024 456 (APC), and The National Research Foundation of Korea, Grant Number 457 2019R1A6A1A10073437 (Y.-N. Lee). We thank the Municipality of Rincon de los 458 Sauces city for supporting the paleontological research projects. We thank Sara Burch 459 for providing photographs of *Majungasaurus*, Matthew Carrano for providing 460 bibliography, and Lucio Ibiricu for comments in the early stages of the manuscript. We 461 also want to thank Federico Agnolín and an anonymous reviewer for their useful 462 comments improved the quality of this contribution. 463 **REFERENCES** 464 Adams, D. C., & Otárola-Castillo, E. (2013). Geomorph: an R package for the 465 collection and analysis of geometric morphometric shape data. Methods in 466 ecology and evolution, 4(4), 393-399. 467 Adams, D. C., Rohlf, F. J., & Slice, D. E. (2013). A field comes of age: Geometric 468 morphometrics in the 21st century. *Hystrix Italian Journal of Mammalogy* 24(1): 469 7-14.

470 Amrhein, V., Trafimow, D., & Greenland, S. (2019). Inferential statistics as descriptive 471 statistics: there is no replication crisis if we don't expect replication. The 472 American Statistician 73:262–70. 473 Benítez, H. A., & Püschel, T. A. (2014). Modelando la varianza de la forma: 474 Morfometría geométrica aplicaciones en biología evolutiva. *International* 475 Journal of Morphology 32: 998–1008. 476 Benjamin, D. J., Berger, J. O., Johannesson, M. et al. (2018). Redefine statistical 477 significance. Nature Human Behaviour 2:6–10. https://doi.org/10.1038/s41562-478 017-0189-z 479 Benton, M. J. (1990). Origin and interrelationships of dinosaurs. In: Weishampel, D. B., 480 Dodson, P., & Osmólska, H. (eds.). The Dinosauria. University of California 481 Press, Berkeley. Pp. 11–30. 482 Bonaparte, J. F. (1985). A horned Cretaceous carnosaur from Patagonia. National 483 Geographic Research 1: 149-151. 484 Bonaparte, J. F. (1991). Los vertebrados fósiles de la Formación Río Colorado, de la 485 ciudad de Neuquén y cercanías, Cretácico superior, Argentina. Revista del 486 Museo Argentino de Ciencias Naturales: Paleontología 4(3): 17–123. 487 Bonaparte, J. F., & Novas, F. E. (1985). Abelisaurus comahuensis, n. g., n. sp., 488 Carnosauria del Cretácico Tardío de Patagonia. Ameghiniana 21(2-4), 259–265. 489 Burch, S. H. (2014). Complete forelimb myology of the basal theropod dinosaur Tawa hallae based on a novel robust muscle reconstruction method. Journal of 490 491 Anatomy, 225(3), 271-297. 492 Burch, S. H. (2017). Myology of the forelimb of Majungasaurus crenatissimus 493 (Theropoda, Abelisauridae) and the morphological consequences of extreme 494 limb reduction. Journal of Anatomy 231(4): 515-531.

495	Burch, S. H., & Carrano, M. 1. (2012). An articulated pectoral girdle and forelimb of
496	the abelisaurid theropod Majungasaurus crenatissimus from the Late Cretaceous
497	of Madagascar. Journal of Vertebrate Paleontology 32(1): 1–16.
498	https://doi.org/10.1080/02724634.2012.622027.
499	Carrano, M. T. (2007). The appendicular skeleton of Majungasaurus crenatissimus
500	(Theropoda: Abelisauridae) from the Late Cretaceous of Madagascar. Society of
501	Vertebrate Paleontology Memoir 8: 163–179.
502	Carrano, M. T., & Sampson, S. D. (2008). The phylogeny of the Ceratosauria
503	(Dinosauria: Theropoda). Journal of Systematic Palaeontology 6: 183-236.
504	Carrano, M. T., Loewen, M. A., & Sertich, J. J. W. (2011). New materials of
505	Masiakasaurus knopfleri Sampson, Carrano & Forster 2001, and implications
506	for the morphology of the Noasauridae (Theropoda: Ceratosauria). Smithsonian
507	Contributions to Paleobiology 95 (pp. viii + 53). 10.5479/si.00810266.95.1.
508	Carrano, M. T., Sampson, S. D., & Forster, C. A. (2002). The osteology of
509	Masiakasaurus knopfleri, a small abelisauroid (Dinosauria: Theropoda) from the
510	Late Cretaceous of Madagascar. Journal of Vertebrate Paleontology 22: 510-
511	534. Charig, A. J., & Milner, A. C. (1997). Baryonyx walkeri, a fish-eating
512	dinosaur from the Wealden of Surrey. Bulletin of the Natural History Museum,
513	Geology Series 53: 11–70.
514	Collyer, M. L., & Adams, D. C. (2018). RRPP: An R package for fitting linear models
515	to high-dimensional data using residual randomization. Methods in Ecology and
516	Evolution 9: 1772-1779.
517	Coria, R. A., Chiappe, L. M., & Dingus, L. (2002). A new close relative of Carnotaurus
518	sastrei Bonaparte 1985 (Theropoda: Abelisauridae) from the Late Cretaceous
519	from Patagonia. Journal of Vertebrate Paleontology 22(2): 460-465.

520	Cruzado-Caballero, P., Filippi, L. S., Méndez, A. H., Garrido, A. C., & Díaz-Martínez,
521	I. (2018). First ornithopod remains from the Bajo de la Carpa Formation
522	(Santonian, Upper Cretaceous), northern Patagonia, Argentina. Cretaceous
523	Research 83: 182-193.
524	Cruzado-Caballero, P., Gasca, J. M., Filippi, L. S., Cerda, I. A., & Garrido, A. C.
525	(2019). A new ornithopod dinosaur from the Santonian of Northern Patagonia
526	(Rincón de los Sauces, Argentina). Cretaceous Research 98: 211-229.
527	Filippi, L. S., Juárez-Valieri, R. D., Gallina, P. A., Méndez A. H., Gianechini, F. A., &
528	Garrido, A. C. (2024). A rebbachisaurid-mimicking titanosaur and evidence of a
529	Late Cretaceous faunal disturbance event in South-West Gondwana. Cretaceous
530	Research 154: 105754. https://doi.org/10.1016/j.cretres.2023.105754
531	Filippi, L. S., Méndez, A. H., Juárez-Valieri, R. D., & Garrido, C. A. (2016). A new
532	brachyrostran with hypertrophied axial structures reveals an unexpected
533	radiation of latest Cretaceous abelisaurids. Cretaceous Research 61: 209-219.
534	Filippi, L. S.; Barrios, F.; & Garrido, A. C. (2018). A new peirosaurid from the Bajo de
535	la Carpa Formation (Upper Cretaceous, Santonian) of Cerro Overo, Neuquén,
536	Argentina. Cretaceous Research 83: 75-83.
537	Gianechini, F. A., Apesteguía, S., Landini, W., Finotti, F., Juarez-Valieri, R. D., &
538	Zandonai, F. (2015). New abelisaurid remains from the Anacleto Formation
539	(Upper Cretaceous), Patagonia, Argentina. Cretaceous Research 54: 1–16.
540	Gianechini, F. A., Filippi, L. S., Méndez, A. H., & Garrido, A. C. (2022). A non-
541	furileusaurian caudal vertebra from the Bajo de la Carpa Formation (Upper
542	Cretaceous, Santonian) and morphological variation in the tail of Abelisauridae.
543	Publicación Electrónica de la Asociación Paleontológica Argentina 22(2): 58–
544	70.

545	Gianechini, F. A., Méndez, A. H., Filippi, L. S., Paulina-Carabajal, A., Juárez-Valieri,
546	R. D., & Garrido, C. A. (2021). A new furileusaurian abelisaurid from La
547	Invernada (Upper Cretaceous, Santonian, Bajo de la Carpa Formation), northern
548	Patagonia, Argentina. Journal of Vertebrate Paleontology 40(6).
549	https://doi.org/10.1080/02724634.2020.1877151
550	Holtz, T. R. Jr. (2000). A new phylogeny of the carnivorous dinosaurs. GAIA 15: 5-61.
551	Janensch, W. (1920). Ueber Elaphrosaurus bambergi und die Megalosaurier aus den
552	Tendaguru-Schichten Deutsch-Ostafrikas. Sitzungsberichte der Gesellschaft
553	naturforschender Freunde zu Berlin: 225–235.
554	Jasinoski, S. C., Russell, A. P., & Currie, P. J. (2006). An integrative phylogenetic and
555	extrapolatory approach to the reconstruction of dromaeosaur (Theropoda:
556	Eumaniraptora) shoulder musculature. Zoological Journal of the Linnean
557	Society 146: 301–344.
558	Jiménez-Gomis, C., Cruzado-Caballero, P., Gasca, J. M., & Filippi, L. S. (2018). New
559	fossils of ornithopod dinosaurs from the Santonian (Upper Cretaceous) of the
560	Bajo de la Carpa Formation of North Patagonia (Neuquén, Argentina).
561	Geogaceta 64: 83-86.
562	Langer, M. A., Martins, N., Manzig, P. C., Ferreira, G., Marsola, J. C., Fortes, E., Lima
563	R., Sant'ana, L. C. F., Vidal, L., Lorençato, R., & Ezcurra, M. D. (2019). A new
564	desert-dwelling dinosaur (Theropoda, Noasaurinae) from the Cretaceous of
565	south Brazil. Scientific Reports 9, 9379. https://doi.org/10.1038/s41598-019-
566	45306-9
567	Lavocat, R. (1955). Sur une portion de mandibule de théropode provenant du Crétacé
568	supérieur de Madagascar. Bulletin du Muséum de l'Histoire Naturelle, Paris, 2e
569	série, 27: 256–259.

570 Madsen Jr., J. H. (1976). Allosaurus fragilis: a revised osteology. Utah Geological and 571 Mining Survey Bulletin 109: 1–163. 572 Madsen Jr., J. H., & Welles, S. P. (2000). Ceratosaurus (Dinosauria, Theropoda) a 573 Revised Osteology. *Utah Geological Survey, Miscellaneous Publication 00-2*: 1-574 80. 575 Marsh, O. C. (1881). Principal characters of American Jurassic dinosaurs. Part V. The 576 *American Journal of Science and Arts 3*(21): 417–423. 577 Marsh, O. C. (1884). Principal characters of American Jurassic dinosaurs. Part VIII. 578 The order Theropoda. American Journal of Science 27: 329–340. 579 Méndez, A. H., Fernández, M. S., & Filippi, L. S. (2024). First record of non-avian 580 theropod eggs from La Invernada fossil site (Bajo de la Carpa Formation, 581 Santonian), Rincón de los Sauces, Neuquén, Argentina. Publicación Electrónica 582 de la Asociación Paleontológica Argentina 24(R3): 108R. 583 Méndez, A. H., Novas, F. E., & Chatterjee, S. (2010). An abelisaurid humerus from the 584 Upper Cretaceous of India. Paläontologische Zeitschrift 84: 421-425. 585 Méndez, A. H., Filippi, L. S., Gianechini, F. A., & Juárez-Valieri, R. D. (2018). New 586 brachyrostran remains (Theropoda, Abelisauridae) from La Invernada fossil site 587 (Bajo de la Carpa Formation, Upper Cretaceous), northern Patagonia, Argentina. 588 Cretaceous Research 83: 120-126. 589 Méndez, A. H., Gianechini, F. A., Paulina-Carabajal, A., Filippi, L. S., Juárez-Valieri, 590 R. D., Cerda, I. A., & Garrido, C. A. (2022). New furileusaurian remains from 591 La Invernada (Northern Patagonia, Argentina): a site of unusual abelisaurids 592 abundance. Cretaceous Research 129: 104989. 593 https://doi.org/10.1016/j.cretres.2021.104989

594	Novas, F. E., Ezcurra, M. D., & Agnolín, F. L. (2006). Humerus of a basal abelisauroid
595	theropod from the Late Cretaceous of Patagonia. Revista del Museo Argentino
596	de Ciencias Naturales ''Bernardino Rivadavia'' 8(1): 63–68.
597	Novas, F. E., Chatterjee, S., Rudra, D. K., & Datta, P. M. (2010). Rahiolisaurus
598	gujaratensis, n. gen. n. sp., a new abelisaurid theropod from the Late Cretaceous
599	of India. In S. Bandyopadhyay (ed.), New aspects of Mesozoic biodiversity (pp.
600	45–62). Springer Verlag.
601	Panzeri K. M., Gouiric-Cavalli S., Cione A. L., & Filippi L. S. (2022). Description of
602	the first Cretaceous (Santonian) articulated skeletal lungfish remains from South
603	America, Argentina. Comptes Rendus Palevol 21(37): 815-835.
604	Paul, G. S. (1984). The archosaurs: A phylogenetic study. In: Reif, WE., and
605	Westphal, F. (eds.). Third Symposium on Mesozoic Terrestrial Ecosystems,
606	Short Papers. Attempto Verlag, Tübingen. Pp. 175–180.
607	Paulina-Carabajal, A., Díaz-Martínez, I., Ulloa-Guaiquin, K., Méndez, A. H., Filippi, L.
608	S., Gianechini, F. A., González-Dionis, J., Garrido, A. C., Lee, Y-N., & Kim, D-
609	K. (2024). Report of Cretaceous dinosaur natural tracks with skin impressions at
610	the site Cerro Overo, Northern Patagonia. Publicación Electrónica de la
611	Asociación Paleontológica Argentina 24(R2): 21R.
612	Pol, D., & Rauhut, O. W. M. (2012). A Middle Jurassic abelisaurid from Patagonia and
613	the early diversification of theropod dinosaurs. Proceedings of the Royal Society
614	London B 279: 3170–3175.
615	Rauhut, O. W. M. (2003). The interrelationships and evolution of basal theropod
616	dinosaurs. Special Papers in Palaeontology 69: 1–213.

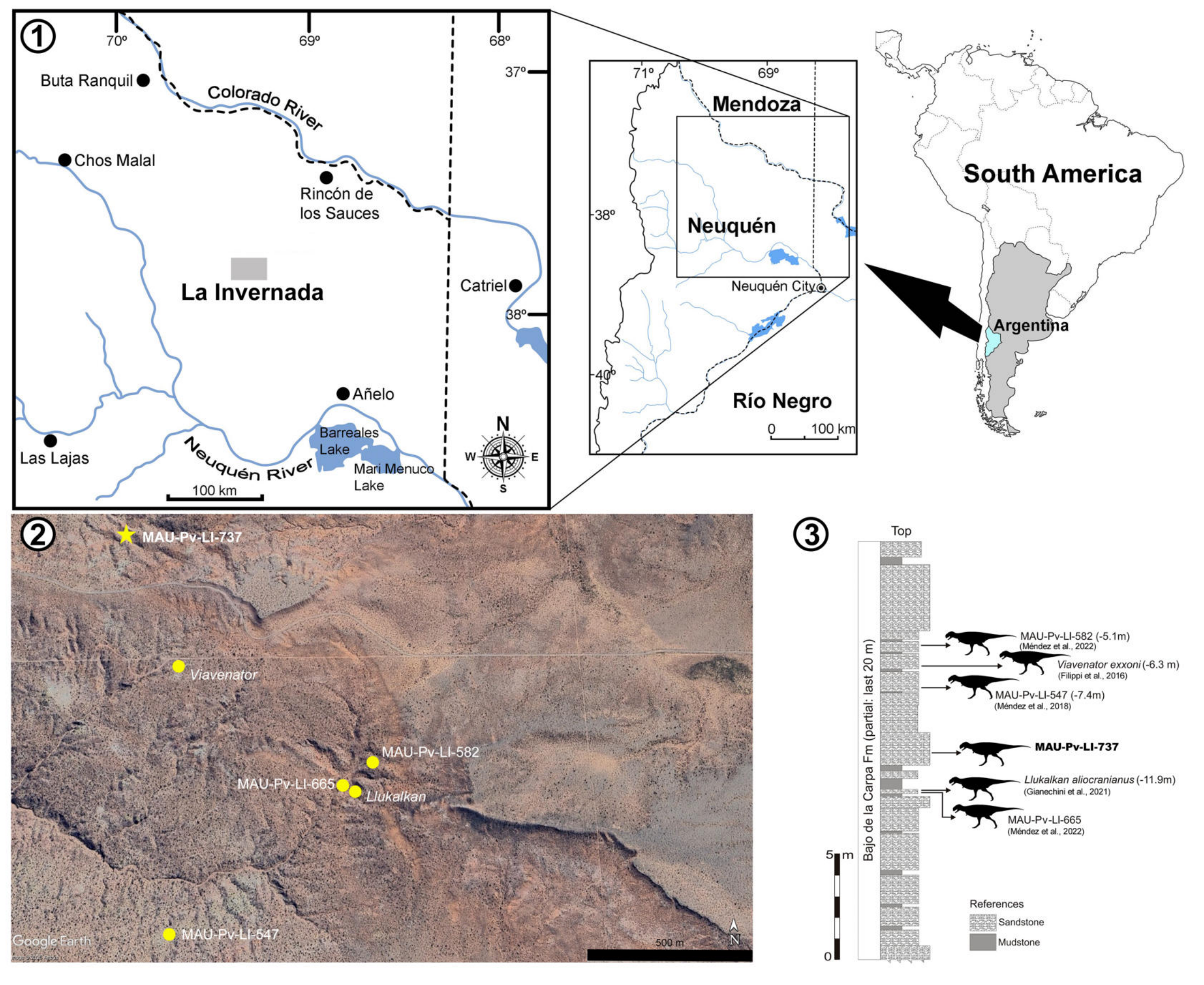
617 Rauhut, O. W. M., & Carrano, M.T. (2016). The theropod dinosaur *Elaphrosaurus* 618 bambergi Janensch 1920, from the Late Jurassic of Tendaguru, Tanzania. 619 Zoological Journal of the Linnean Society, 178(3): 546–610. 620 Rohlf, F. J. (2004). TpsDig. Department of Ecology and Evolution, State University of 621 New York, Stony Brook, NY. 622 Sampson, S. D., Carrano, M. T., & Forster, C. A. (2001). A bizarre predatory dinosaur 623 from the Late Cretaceous of Madagascar. Nature 409: 504-506. 624 Senter, P. J. (2023). Restudy of shoulder motion in the theropod dinosaur *Mononykus* 625 olecranus (Alvarezsauridae). PeerJ, 11, e16605. 626 Senter, P., & Parrish, J. M. (2006). Forelimb function in the theropod dinosaur 627 Carnotaurus sastrei, and its behavioral implications. PaleoBios, 26(3): 7-17. 628 Senter, P., & Robins, J. H. (2005). Range of motion in the forelimb of the theropod 629 dinosaur Acrocanthosaurus atokensis, and implications for predatory 630 behaviour. Journal of Zoology, 266(3), 307-318. 631 Sereno, P. C. (1999). The evolution of dinosaurs. Science 284: 2137–2147. Sereno, P. C., Wilson, J. A. & Conrad, J. L. (2004). New dinosaurs link southern 632 633 landmasses in the mid-Cretaceous. *Proceedings of the Royal Society of London*, 634 Series B 271: 1325–1330. 635 Witmer, L. M. (1995). The extant phylogenetic bracket and the importance of 636 reconstructing soft tissues in fossils. In J. J. Thomason (ed.), Functional morphology in vertebrate paleontology (pp. 19-33). Cambridge University 637 638 Press. 639 Yang, Y., Sánchez-Tójar, A., O'Dea, R. E., Noble, D. W. A., Koricheva, J., Jennions, 640 M. D. Parker, T. H., Lagisz, M., & Nakagawa, S. (2023). Publication bias

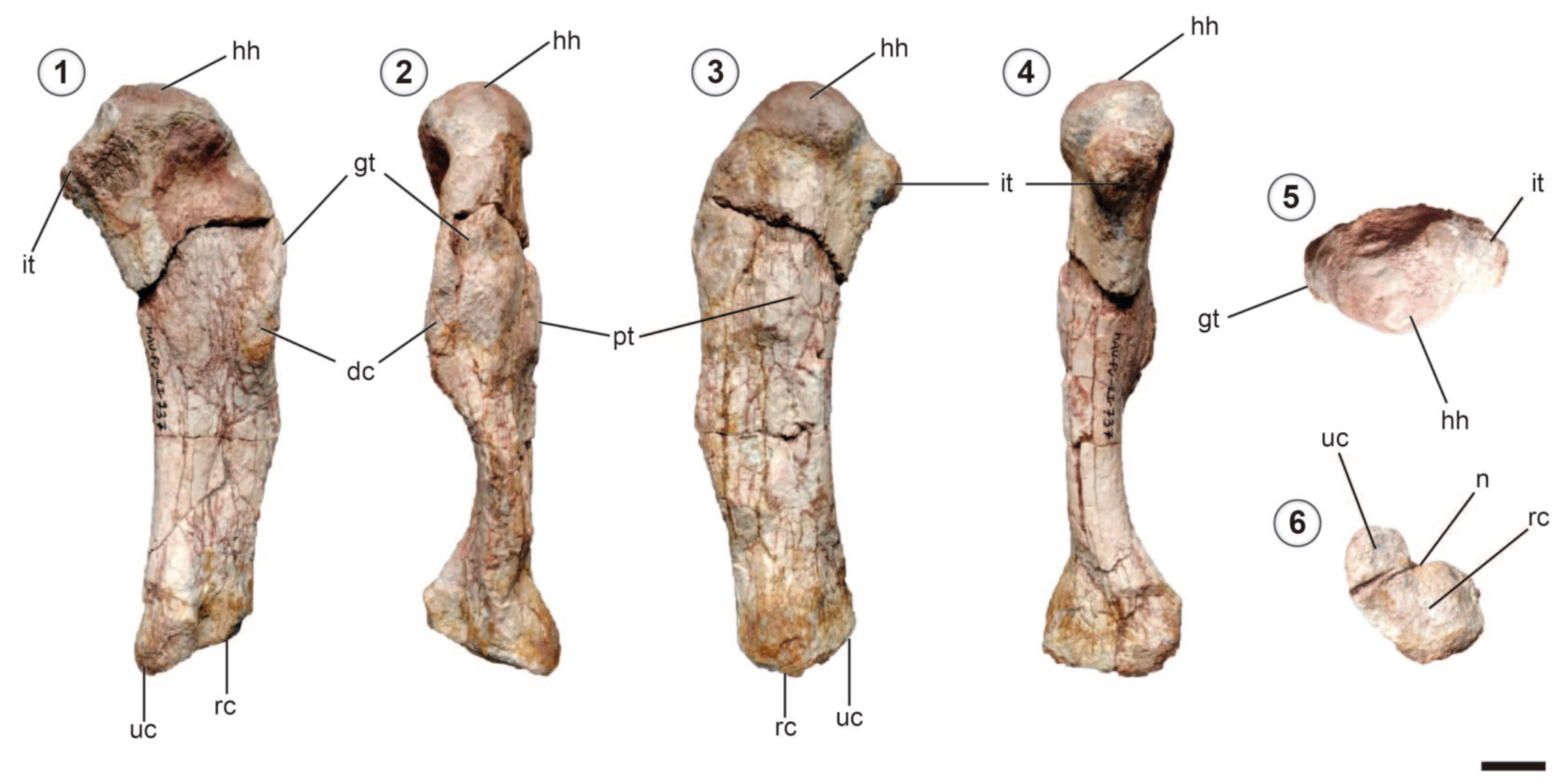
impacts on effect size, statistical power, and magnitude (Type M) and sign

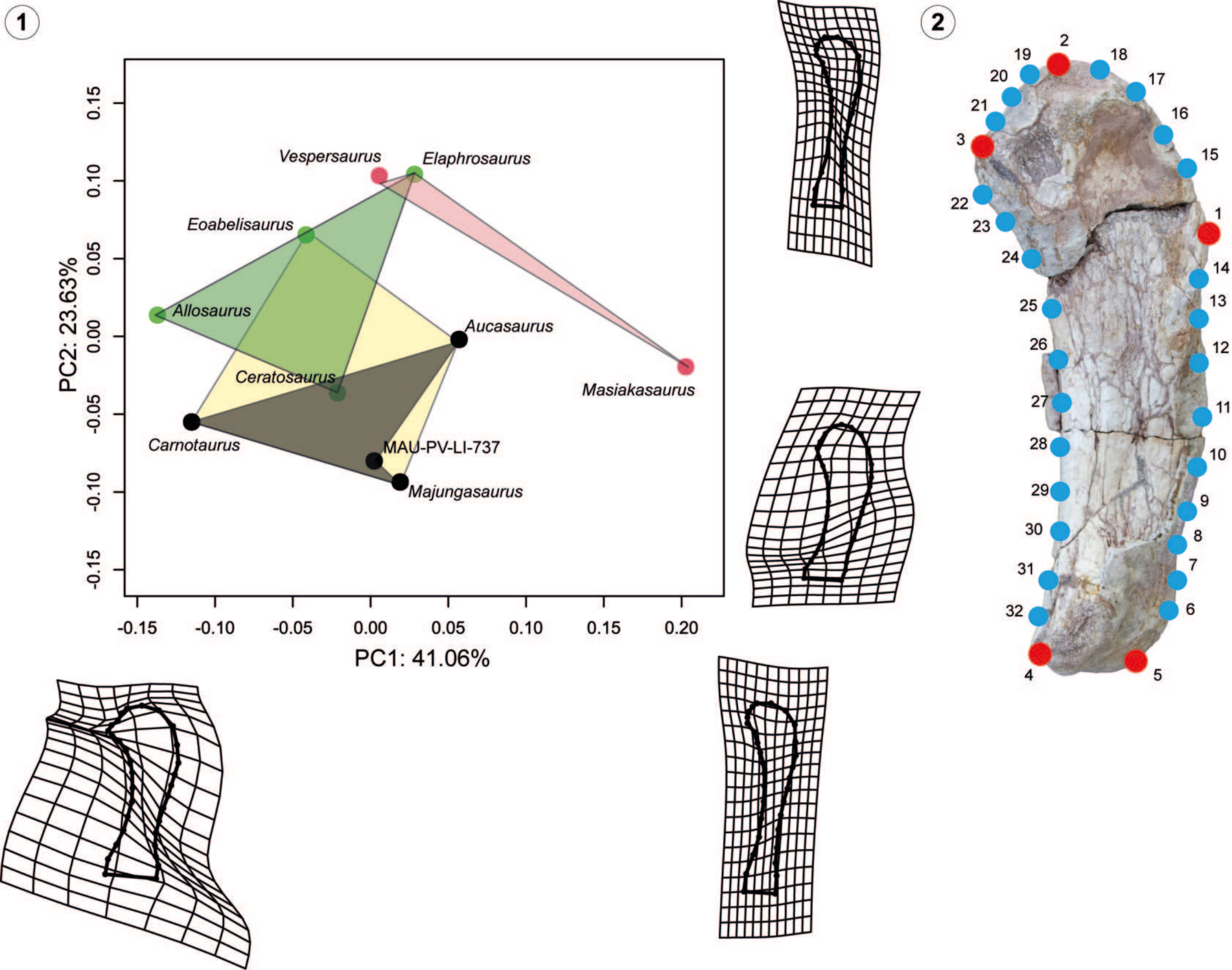
642	(Type S) errors in ecology and evolutionary biology. <i>BMC Biology 21:/</i> 1
643	https://doi.org/10.1186/s12915-022-01485-y
644	Zelditch, M. L., Swiderski, D. L., Sheets, H. D., & Fink, W. L. (2004). Geometric
645	morphometrics for biologists: a primer. Elsevier Academic Press, San Diego.
646	https://doi.org/10.1016/B978-0-12-778460-1.X5000-5
647	
648	Appendices
649	Figure captions
650	Figure 1. (1) Map of the location of the La Invernada fossil area. (2) Detailed map
651	showing the spatial provenance of the abelisaurid specimens of La Invernada. (3)
652	Stratigraphic column with the location of the different finds (Modified from Méndez et
653	al., 2022).
654	
655	Figure 2. MAU-PV-LI-737 left humerus in (1) anterior, (2) lateral, (3) posterior, (4)
656	medial, (5) proximal, and (6) distal views. Abbreviations: dc, deltopectoral crest; gt,
657	greater tubercle; hh, humeral head; it, internal tuberosity; n, notch; pt, posterior
658	tuberosity; rc , radial condyle; uc , ulnar condyle. Scale bar equals 20 mm.
659	
660	Figure 3: 1) PCA showing the first two Principal Components (PC) and deformation
661	grids representing the shape of each extreme of the axis. The ratios represent the
662	variance explained by each PC. Color areas delimits the morphospace occupied by Late
663	Cretaceous abelisaurids (black), Abelisauridae (yellow), Jurassic taxa (green) and
664	Noasauridae (red). 2) Landmark configuration over MAU-PV-LI-737 used in the
665	analyses, in which landmarks are in red and semilandmarks are in blue.
666	

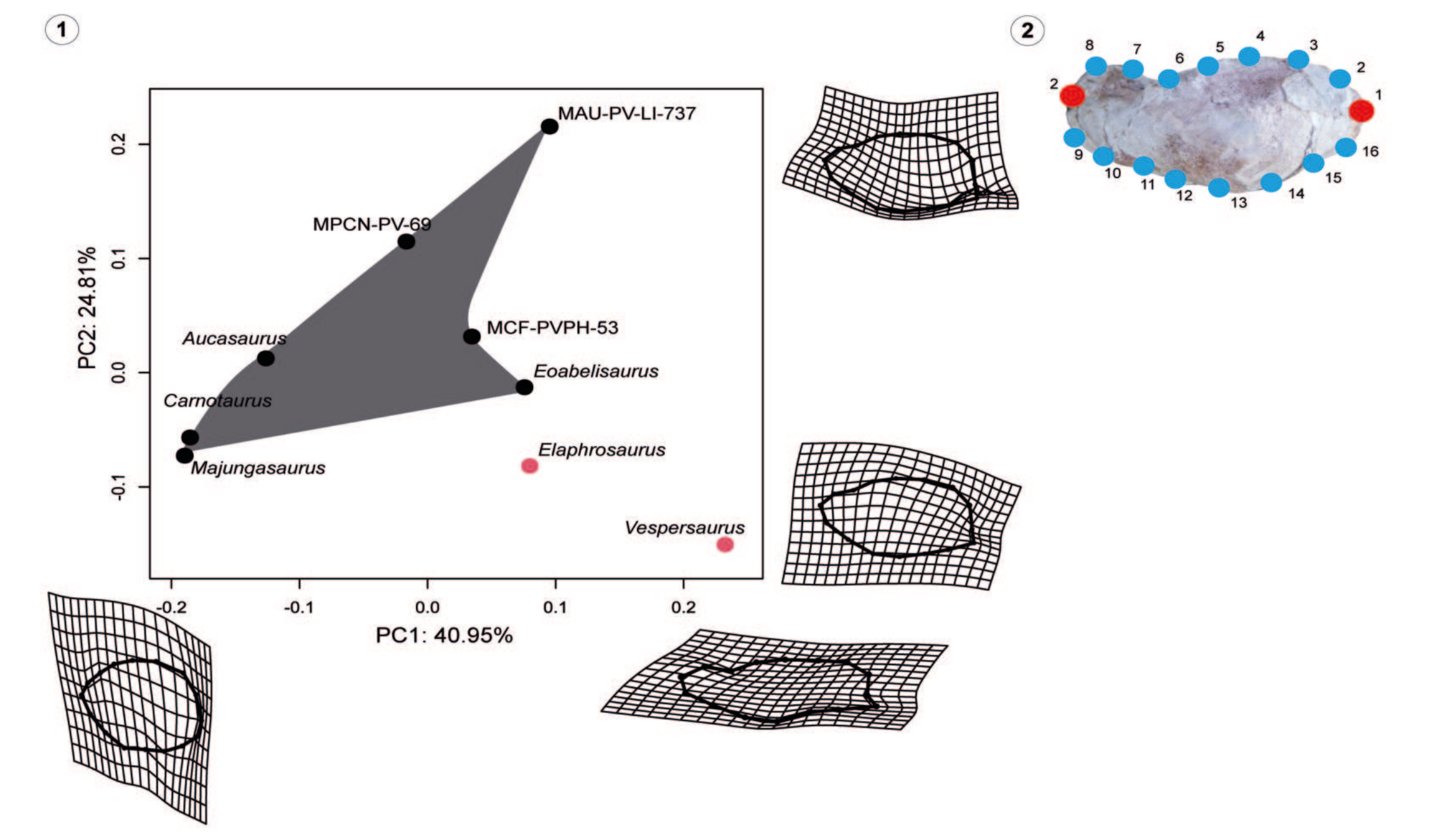
Figure 4. 1) PCA showing the first two Principal Components (PC) and deformation 667 668 grids representing the shape of each extreme of the axis. The ratios represent the 669 variance explained by each PC. Color area delimits the morphospace occupied by 670 abelisaurids (black). 2) Landmark configuration over MAU-PV-LI-737 used in the 671 analyses, in which landmarks are in red and semilandmarks are in blue. 672 673 Figure 5. Myological reconstruction of the humerus of MAU-PV-LI-737 in anterior (1), 674 lateral (2), posterior (3), and medial (4) views. Proposed muscle origins are indicated in 675 red, proposed insertions in blue. Abbreviations: AN, M. anconeus; AR, M, abductor 676 radialis; **BB**, M. biceps brachii; **BR**, M. brachialis; **CB**, M. coracobrachialis; 677 **DC**, M. deltoideus clavicularis; **DS**, M. deltoideus scapularis; **EA**, M. 678 epitrocheloanconeus; ECR, M. extensor carpi radialis; ECU, M. extensor carpi 679 ulnaris; **EDL**, M. extensor digitorum longus; **FCU**, M. flexor carpi ulnaris; **FDLS**, M. 680 flexor digitorum longus superficialis; LD, M. latissimus dorsi; P, M. pectoralis; PT, M. 681 pronator teres; SBC, M. subcoracoideus; SBS, M. subscapularis; SC, M. 682 supracoracoideus; SCA, M. supracoracoideus accessorius; SHP, M, scapulohumeralis 683 posterior; SU, M. supinator; TBL, M. triceps brachii longus; TBM, M. triceps brachii 684 medialis. Scale bar: 20mm. 685 686 **Figure 6.** Humeri of several abelisauroid theropods in anterior (1-9), lateral (10-18), 687 and proximal (19-27) views. (1,10,19) Masiakasaurus (FMNH PR 2485 from Carrano 688 et al., 2011); (2,11,20) Elaphrosaurus (MB R 4960 from Rauhut & Carrano, 2016); 689 (3,12,21) Vespersaurus (MPCO.V 0006d from Langer et al., 2019); (4,13,22) MCF-690 PVPH 53 (from Novas et al., 2006); (5,14,23) MAU-PV-LI-737; (6,15,24) 691 Rahiolisaurus (ISIR 657 from Méndez et al., 2010); (7,16,25) Majungasaurus (FMNH

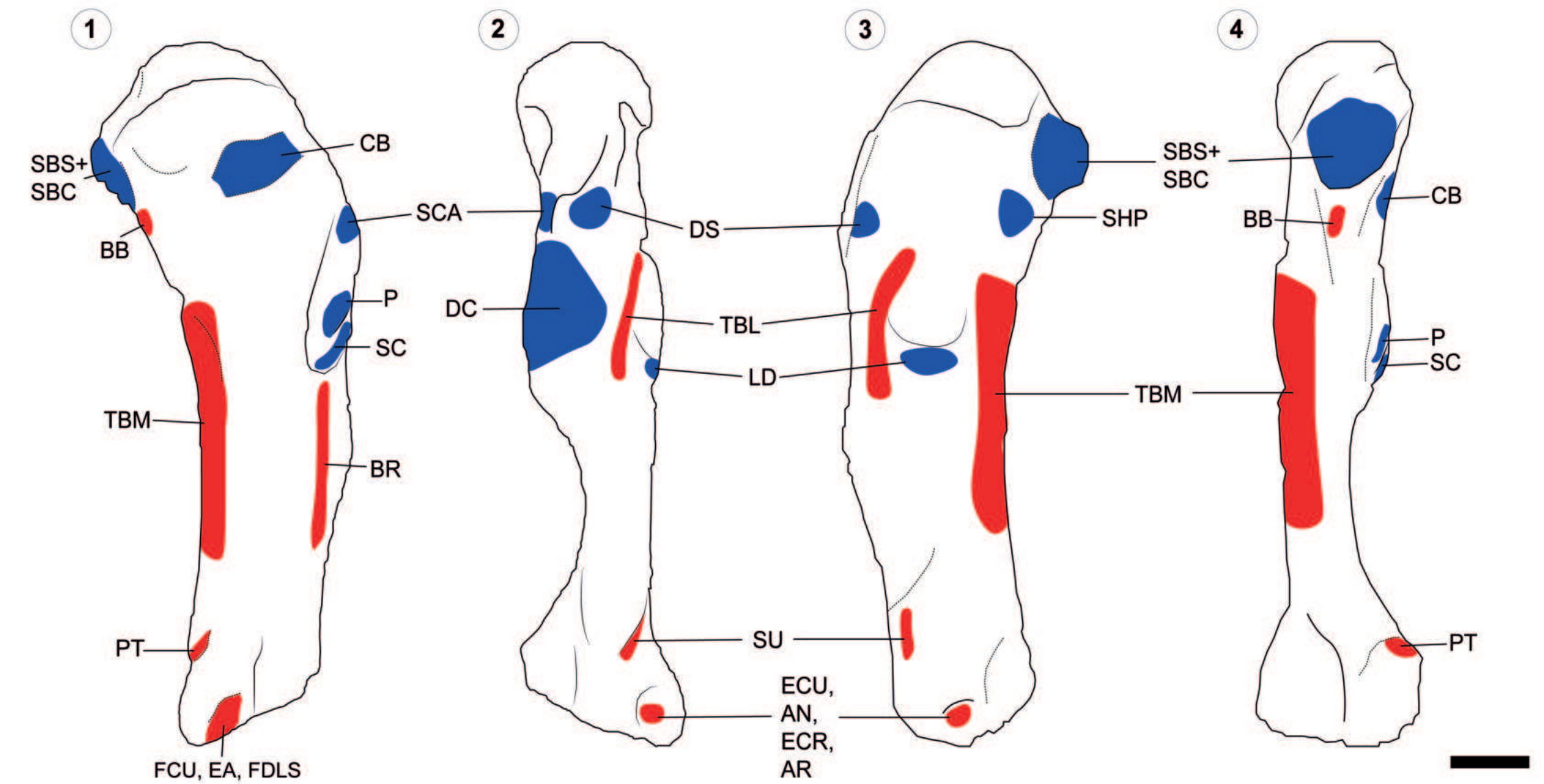
- 692 PR 2423 from Carrano, 2007; FMNH PR 2836 from Burch & Carrano, 2012); (8,17,26)
- 693 MPCN-PV-69; (9,18,27) *Carnotaurus* (MACN-CH 894). Not to scale.











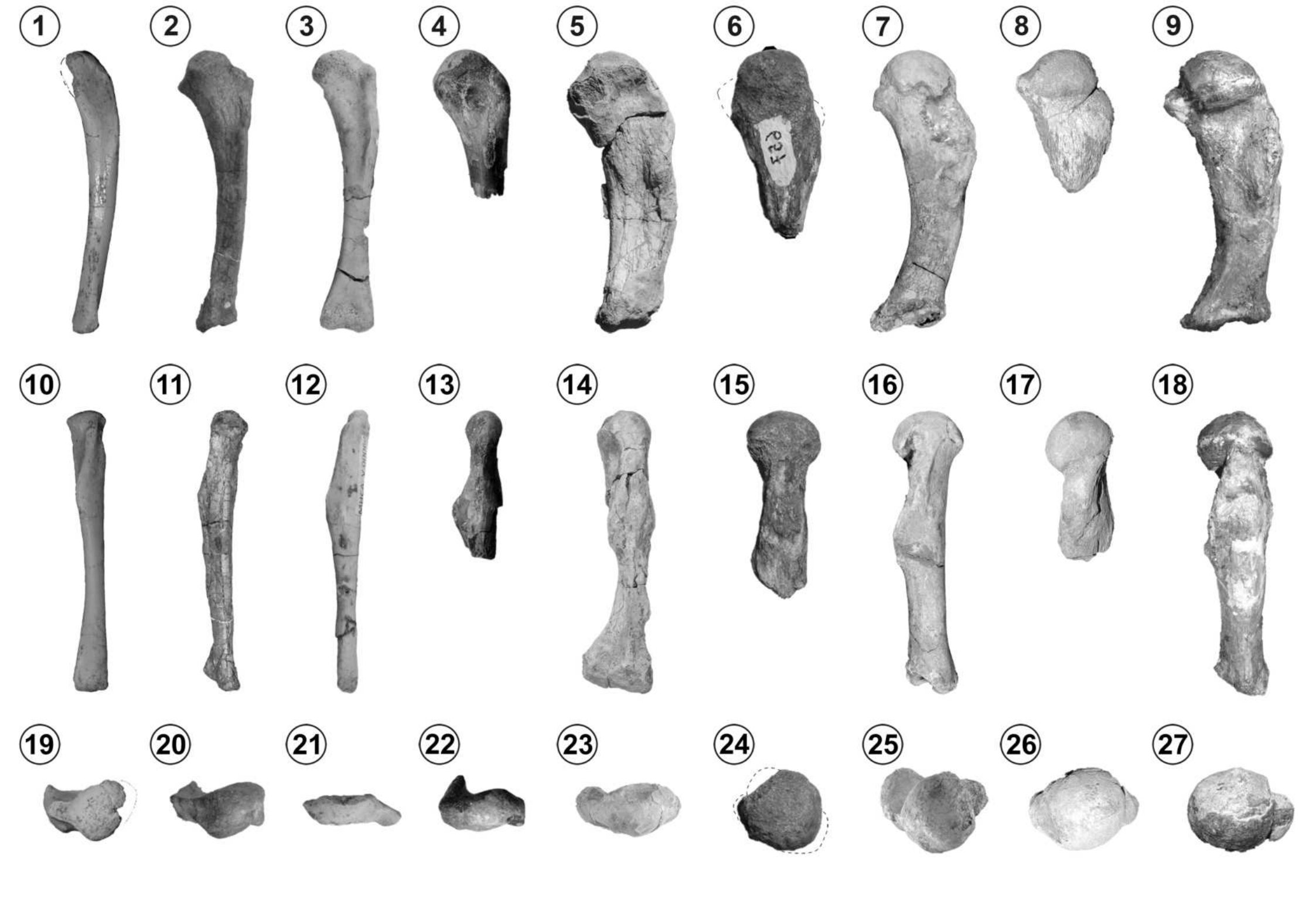


TABLE 1. Procrustes ANOVA performed in Procrustes coordinates and 90% of PCA. Variables: Taxonomy (Abelisauridae, early diverging taxa and Noasauridae), Size of humeri and the interaction between the Taxonomy and size (Taxonomy*Size). SS: sum of square. R2: Variance explained by the factor in data. Z: effect of size.

SS	R2	Z	SS	R2	Z
0.06	0.30	1.06	0.04	0.31	0.59
0.02	0.09	0.15	0.01	0.09	0.10
0.03	0.16	-0.23	0.01	0.15	-0.42
0.07	0.38		0.05	0.36	
0.19			0.13		
	0.06 0.02 0.03 0.07	0.06 0.30 0.02 0.09 0.03 0.16 0.07 0.38	0.06 0.30 1.06 0.02 0.09 0.15 0.03 0.16 -0.23 0.07 0.38	0.06 0.30 1.06 0.04 0.02 0.09 0.15 0.01 0.03 0.16 -0.23 0.01 0.07 0.38 0.05	0.06 0.30 1.06 0.04 0.31 0.02 0.09 0.15 0.01 0.09 0.03 0.16 -0.23 0.01 0.15 0.07 0.38 0.05 0.36